

Power factor correction of synchronous motor using hybrid fuzzy control system

Hung Quoc Duong¹, Dung Thi To²

¹Department of Automation, Faculty of Electrical Engineering, Thai Nguyen university of Technology, Viet Nam

²Experimental center, Thai Nguyen university of Technology, Viet Nam

Date of Submission: 10-05-2023

Date of Acceptance: 23-05-2023

ABSTRACT: Synchronous motors are known for two basic tasks. The first, it is an efficient device for converting electrical energy into mechanical energy. The second, it can work as a reactive power compensator to improve the power factor of the grid, by adjusting the excitation source supplied to the rotor windings of the motor. This paper presents the application of hybrid fuzzy system to excitation control system for synchronous motor. Hybrid fuzzy system with cascade structure, including: PI controller, in which the Ziegler-Nichols method combined with trial and error is used to determine the controller's parameters. The fuzzy controller has the function of compensating the control signal for the PI controller. The simulation results show that the system meets the power factor correction of the setpoint.

KEYWORDS: Synchronous motor; Excitation system ; Ziegler nichols method; Trial and error method; Hybrid fuzzy control system.

I. INTRODUCTION

The power factor correction of the synchronous motor is performed on the rotor side by the excitation regulator. This is useful in applications where the motor is subjected to transient effects at heavy loads. The synchronous motor excitation regulator must measure the power factor drop that occurs when the motor is subjected to sudden heavy load and send a signal to the thyristor static rectifier to increase the value of the DC source, this process is called forging. As a result, the torque of the synchronous motor is increased during transient loads [1-2]. In addition, the voltage drop of the power grid must also be recognized by the controller and have a solution to adjust the field current [3 - 4]. Another application of the power factor regulator is to control the power factor variation of the plant caused by asynchronous motors, thereby improving the voltage quality of the plant [5 - 6].

PID control theory is widely applied to excitation systems [4], [7], [8]. With the system PID controller for fast response, but the response is still not good when transient. The solution using fuzzy controller is also used to improve the quality of excitation control system. The simulation results show that the fuzzy controller has a good response, but the response speed is slower than that of the PID [9-10].

The hybrid between PID controller and fuzzy control has been widely applied in control and has brought about efficiency [11 – 15]. This paper continues to propose a solution to apply hybrid control system between PI controller and fuzzy control to apply excitation regulator in synchronous motor control system. The Ziegler-Nichols method combined with trial and error is used to determine the parameters of the PI controller. The fuzzy controller has the function of compensating the control signal at the output of the PI controller. The simulation results show that the hybrid fuzzy controller gives better response than the PI with Ziegler-Nichols or PI with trial and error.

II. PROBLEM DESCRIPTION

2-1-Excitation system of large synchronous motor

For a large synchronous motor, the power supply to the stator is usually a medium voltage grid, 6kV. The excitation source for the motor is usually a low voltage grid, 380V, which is lowered to the appropriate voltage level through a rectifier transformer. This power supply is then rectified to direct current to supply excitation current to the motor. To stabilize the working mode of the motor, the power factor stabilization plays a crucial role. Therefore, an excitation controller is designed aiming to stabilize the power factor $\cos\phi$. The block diagram of the excitation control system for a synchronous motor is shown in Figure 1.

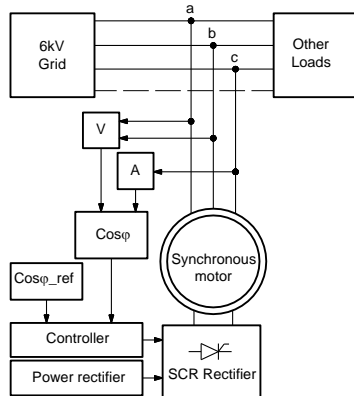


Figure 1. Block diagram of excitation control for synchronous motor.

The phase difference between voltage and current is measured and compared to a desired $\cos\phi$. The controller then calculates a control signal, which is sent to the rectifier to adjust the excitation current in order to achieve the desired power factor. To ensure favorable measurement of the phase difference between voltage and current, the stator windings of the synchronous motor can be star or delta connected to the grid. A typical power factor measurement method is to measure the angle of the voltage between two phases and the current of the other phase, as shown in Figure 2. The figure demonstrates that u_{ab} is 90° earlier than i_{sc} . Therefore, when calculating the phase difference angle between voltage and current, ϕ , the stator must shift the angle of u_{sab} by an angle of 90° to coincide with the angle of i_{sc} .

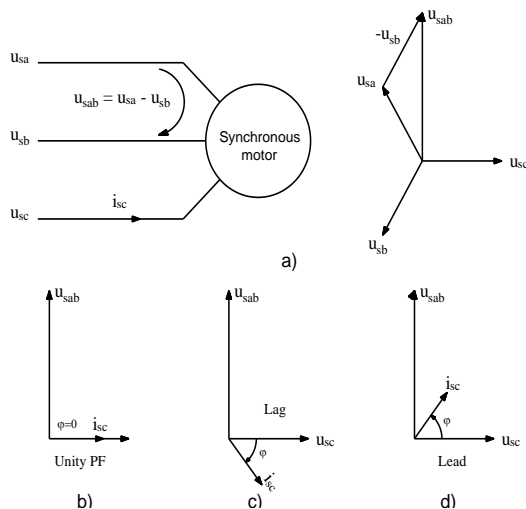


Figure 2. Vector diagram of stator current and voltage: (a) Vector diagram of stator current; (b) current and voltage are in same phase; (c) current lags behind voltage in phase; and (d) current leads ahead of voltage in phase.

2-2- Motor modelling

In this section, the backgrounds of the synchronous motor modelling are presented to demonstrate the critical role of power factor regulation and stabilization.

2-2-1-Motor equations and equivalent circuits

Figure 3 shows a two-axis salient pole synchronous motor in a rotor coordinate system. The frame for stator windings, (α, β) , is stationary with the real axis attached to the stator phase A. Meanwhile, the frame for the excitation and the damper windings, (d, q) , is rotating with the real axis fixed to the center of the pole shoe. This coordinate system rotates with the rotor angular velocity, so both d- and q- magnetic paths are constant. The excitation winding, (f) , is attached on the the d-axis. The damper winding is replaced by two windings in space quadrature, one on the d-axis, (D) , and the other on the q-axis (Q) . The stator three-phase winding is also replaced by two windings in perpendicular space, on the d-axis, (d) , and on the q-axis (q) . The electrical equations of the motor are given as below [16]:

$$u_d = R_s i_d + \frac{d\psi_{sd}}{dt} - \omega_r \psi_{sq}, \quad (1)$$

$$u_q = R_s i_q + \frac{d\psi_{sq}}{dt} + \omega_r \psi_{sd}, \quad (2)$$

$$u_f = R_f i_f + \frac{d\psi_f}{dt}, \quad (3)$$

$$u_D = R_D i_D + \frac{d\psi_D}{dt} = 0, \quad (4)$$

$$u_Q = R_Q i_Q + \frac{d\psi_Q}{dt} = 0, \quad (5)$$

where u_d is the d-axis stator voltage, u_q is the q-axis stator voltage, u_f is the excitation voltage, u_D is the d-axis damper winding voltage, u_Q is the q-axis damper winding voltage, i_d is the d-axis stator current, i_q is the q-axis stator current, i_f is the excitation current, i_D is the d-axis damper winding current, i_Q is the q-axis damper winding current, ψ_d is the d-axis stator flux linkage, ψ_q is the q-axis stator flux linkage, ψ_f is the excitation flux linkage, ψ_D is the d-axis damper winding flux linkage, ψ_Q is the q-axis damper winding flux linkage, $\omega_r = \frac{d\theta}{dt}$ is the angular velocity between

the rotor coordinates and the stationary reference frame α, β , θ_r is the angle between the rotor coordinates and the stationary reference frame.

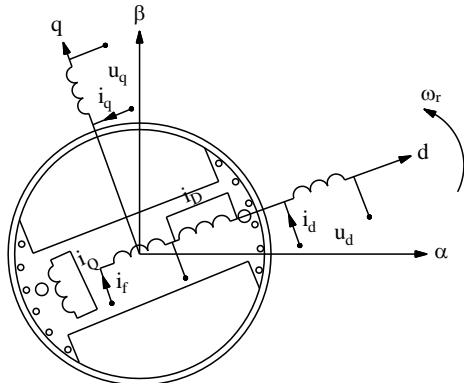


Figure 3. Two-axis salient pole synchronous motor model in the rotor coordinate systems.

The relationship between the motor currents and flux linkages can be defined by using various inductances of the motor [16]:

$$\Psi_{sd} = \Psi_{md} + i_d L_{s\sigma} = L_{md}(i_f + i_d + i_D) + i_d L_{s\sigma}, \quad (6)$$

$$\Psi_{sq} = \Psi_{mq} + i_q L_{s\sigma} = L_{mq}(i_q + i_Q) + i_q L_{s\sigma}, \quad (7)$$

$$\Psi_f = \Psi_{md} + i_f L_{f\sigma} + (i_f + i_D)L_{k\sigma} = L_{md}(i_d + i_D + i_f) + (i_f + i_D)L_{k\sigma} + i_f L_{f\sigma}, \quad (8)$$

$$\Psi_D = \Psi_{md} + i_D L_{D\sigma} + (i_f + i_D)L_{k\sigma} = L_{md}(i_d + i_D + i_f) + (i_f + i_D)L_{k\sigma} + i_D L_{D\sigma}, \quad (9)$$

$$\Psi_Q = \Psi_{mq} + i_Q L_{Q\sigma} = L_{mq}(i_q + i_Q) + i_Q L_{Q\sigma}, \quad (10)$$

where L_{md} is the d-axis magnetising inductance, $L_{s\sigma}$ is the d-axis leakage inductance, $L_{D\sigma}$ is the d-axis damper winding leakage inductance, $L_{f\sigma}$ is the d-axis magnetising winding leakage inductance, $L_{k\sigma}$ is the d-axis Canay inductance, L_{mq} is the q-axis magnetising inductance, $L_{Q\sigma}$ is the q-axis damper winding leakage inductance, R_s is the stator resistance, R_f is the magnetising winding resistance, R_D is the d-axis damper winding resistance, and R_Q is the q-axis damper winding resistance.

From (1)–(10), the equivalent circuits of a synchronous motor can be obtained, as illustrated in Figures 4 and 5.

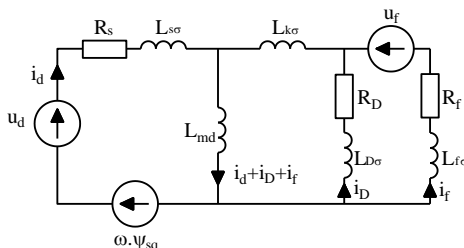


Figure 4. Equivalent circuits of the synchronous motor on the d-axis.

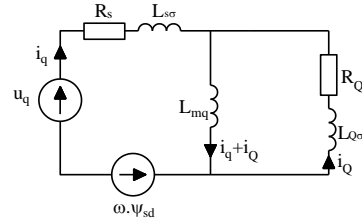


Figure 5. Equivalent circuits of the synchronous motor on the q-axis.

2-2-2-Vector diagram of a synchronous motor

From (1)–(10), the vector diagram of the salient pole synchronous motor is built as shown in Figure 6.

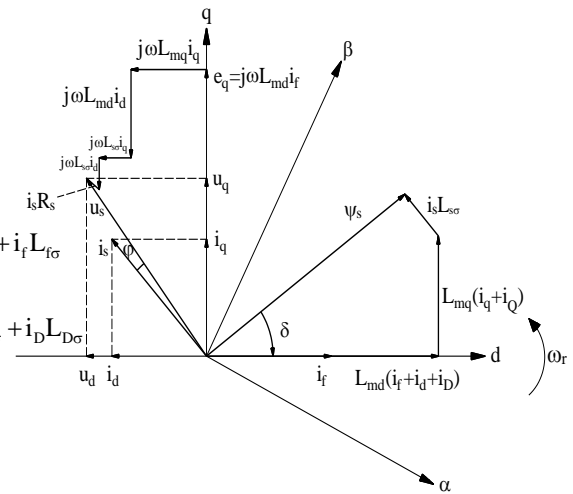


Figure 6. Vector diagram of the salient pole synchronous motor.

In fact, the stator resistance is usually minimal compared to its inductance. Therefore, the voltage drop across the stator resistor can be ignored. The total inductances in the machine are denoted as

$$L_{sd} = L_{s\sigma} + L_{md}, \quad (11)$$

$$L_{sq} = L_{s\sigma} + L_{mq}, \quad (12)$$

$$X_{sd} = \omega L_{sd}, \quad (13)$$

$$X_{sq} = \omega L_{sq}, \quad (14)$$

where X_{sd} and X_{sq} are corresponding d- and q-axis stator reactances. From (11), (12), and Figure 6, assuming that voltage drop on R_s is ignored, we obtain:

$$u_d = j(\omega L_{mq} + \omega L_{s\sigma})i_q = \omega L_{sq} i_q = jX_{sq} i_q \quad (15)$$

$$u_q = e_q + j(\omega L_{md} + \omega L_{s\sigma})i_d = e_q + j\omega L_{sd} i_d = e_q + jX_{sd} i_d \quad (16)$$

$$u_s = u_d + u_q = e_q + jX_{sd} i_d + jX_{sq} i_q = e_q + jX_s i_s \quad (17)$$

where X_s is the stator reactance. From (15)–(17), a simplified vector diagram can be then constructed as shown in Figure 7, with the angle between the voltage vector, u_s , and the q-axis electromotive force, e_q , being the load angle δ .

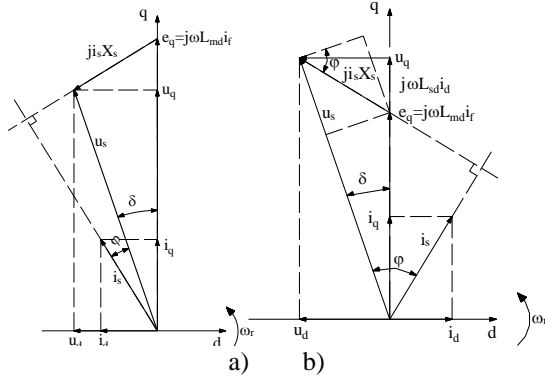


Figure 7. Vector diagram of a synchronous motor in steady-state mode when stator winding resistance is ignored, with $X_s = \omega L_s$: (a) Current leads of voltage in phase, and (b) Current lags behind voltage in phase.

According Figure 7b, we have:

$$I_s X_s \cos \varphi = E_q \sin \delta, \quad (18)$$

Accordingly,

$$U_s I_s \cos \varphi = \frac{U_s E_q \sin \delta}{X_s}. \quad (19)$$

where U_s and I_s are corresponding amplitude of stator voltage and current, E_q is the amplitude of excitation electromotive force, and $X_s = \omega L_s$ is the stator reactance.

The electromagnetic power of the motor, ignoring the losses, is given as below [17]:

$$P_e = P_m = \frac{3}{2} U_s I_s \cos \varphi, \quad (20)$$

where P_e and P_m are corresponding the electromagnetic power and motor power. From (19) and (20), we obtain:

$$P_e = P_m = \frac{3}{2} U_s I_s \cos \varphi = \frac{3}{2} \frac{U_s E_q \sin \delta}{X_s}. \quad (21)$$

Eq. (21) shows the relationship between power and excitation voltage and load angle. Assuming the source voltage and frequency are constant, we will have the following relationship:

$$P_e = P_m = f(I_s \cos \varphi), \quad (22)$$

$$P_e = P_m = f(E_q \sin \delta). \quad (23)$$

2-2-3-Torque equation of synchronous motor at steady state

From the vector diagram in Figure 7b, we have:

$$I_s \cos \varphi = I_q \cos \delta - I_d \sin \delta, \quad (24)$$

We can also compute:

$$I_d = \frac{U_q - E_q}{\omega L_{sd}} = \frac{U_s \cos \delta - E_q}{\omega L_{sd}}, \quad (25)$$

$$I_q = \frac{U_s \sin \delta}{\omega L_{sq}}. \quad (26)$$

Substituting (24)–(26) into (20), we obtain a second method to determine the electromagnetic power of the motor in working mode as:

$$P_e = \frac{3}{2} \frac{U_s E_q}{\omega L_{sd}} \sin \delta + \frac{3}{2} U_s^2 \frac{(L_{sd} - L_{sq})}{\omega L_{sd} L_{sq}} \sin 2\delta. \quad (27)$$

The electromagnetic torque in working mode is calculated as:

$$T_e = \frac{P_e P_r}{\omega} = \frac{3 p_r}{2 \omega} \left[\frac{U_s E_q}{\omega L_{sd}} \sin \delta + U_s^2 \frac{(L_{sd} - L_{sq})}{\omega L_{sd} L_{sq}} \sin 2\delta \right]. \quad (28)$$

Since $\omega L = X$, (28) can be rewritten as:

$$T_e = \frac{3 p_r}{2 \omega} \left[\frac{U_s E_q}{X_{sd}} \sin \delta + U_s^2 \frac{(X_{sd} - X_{sq})}{X_{sd} X_{sq}} \sin 2\delta \right]. \quad (29)$$

In the steady state, the electromagnetic torque of a salient pole synchronous motor has two components. The first part is the main synchronous torque, which depends on the AC voltage and excitation source, $U_s E_q$. The second component is the reluctance torque which depends only on the stator voltage, U_s^2 . Figure 8 depicts the torque–load angle characteristics of a salient pole synchronous motor, where $T_1(\delta)$ is the main synchronous torque, $T_2(\delta)$ is the reluctance synchronous torque, and $T_e(\delta)$ is the total synchronous torque.

From (29), torque regulation is critical so that the motor remains to work safely in the face of a voltage drop of the mains voltage or overload of the torque. To control the torque, we can adjust the field current, resulting in changing $T_1(\delta)$, which is the main synchronous torque.

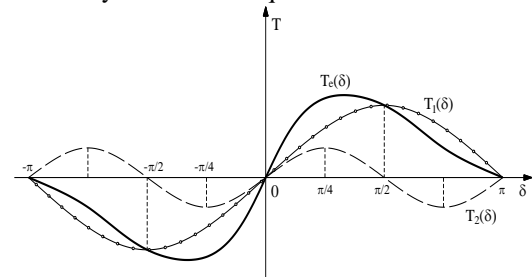


Figure 8. Torque–load angle characteristics of a salient pole synchronous motor.

2-3- Factors affecting the working mode of the motor

For a large synchronous motor, the fluctuation of the load in the operating mode can cause the load angle δ to change accordingly. An excessive change can cause an asynchronous phenomenon, i.e., the rotor magnetic pole slips from the stator magnetic pole. A change in the excitation source can also affect the operating mode of the motor. This section will discuss these effects, in which the load angle, δ , and the current-voltage phase difference, φ , are used to evaluate the operating mode of the motor.

2-3-1-Vector diagram of a synchronous motor

To make it easier to follow, we rotate the coordinate system of the vector diagram so that u_s coincides with the horizontal axis. Assume that the power supply, the power grid frequency, and the DC excitation source are constant. The vector diagram after rotation, in case of load change, is shown in Figure 9.

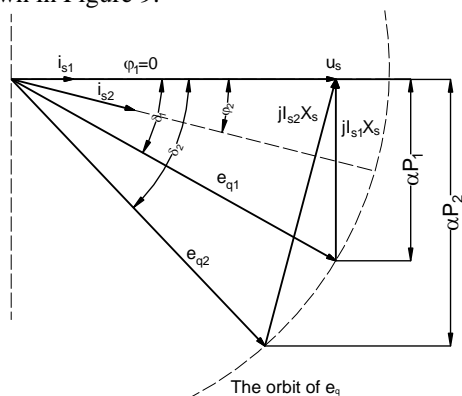


Figure 9. Vector diagram of synchronous motor when stator source and excitation source are constant, load changes from P_1 to P_2 , with $P_2 > P_1$.

According to Figure 9, the motor is initially assumed to work with stator current i_{s1} , power αP_1 , where α is a constant, power factor $\cos\varphi \approx 1$. When the load on the motor shaft increases to αP_2 , the armature current will increase to the value i_{s2} . Assuming the excitation source is constant, its trajectory will draw an arc. Then, the phase difference angle φ increases in the positive direction, $\cos\varphi$ decrease, load angle increases, i.e., $\delta_2 > \delta_1$. When the load δ increases within a permissible range, the stator magnetic field can still lock the rotor magnetic field, so the motor speed remains unchanged. However, if the load increases sharply, δ_2 tends to go to -90° . At this time, the motor is pulled out of synchronous mode. Therefore, the excitation controller must detect a

decrease in the power factor to increase the field current to a suitable value to pull the motor into synchronous mode.

2-3-2-The influence of the excitation source

From (21), if the load and AC source are fixed, then $E_q \sin\delta$ is also a constant. Therefore, when increasing the excitation source E_q , the load angle will decrease. This causes the relative angular position between the rotor and stator magnetic fields to decrease, the stator magnetic poles will be more tightly attached to the rotor, and the motor will run at synchronous speed. The vector diagram when changing the excitation source value is illustrated in Figure 10, therein the subscript {1, 2, 3} are corresponding to three different excitation source values.

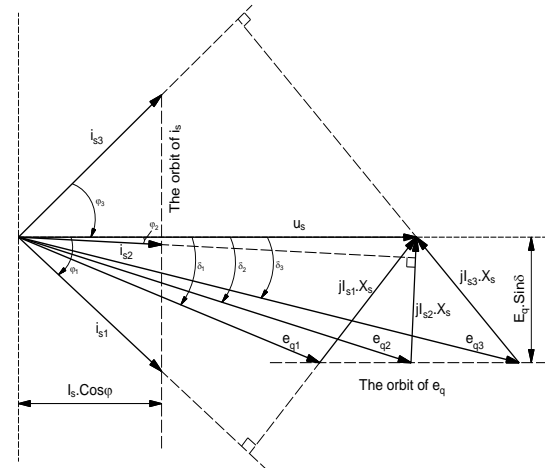


Figure 10. The influence of the excitation source on the working mode.

According to (21), with a fixed load, we have:

$$E_{q1} \sin\delta_1 = E_{q2} \sin\delta_2 = E_{q3} \sin\delta_3 = E_q \sin\delta. \quad (30)$$

From (30) and Figure 10 we see that the trajectory of E_q will slide parallelly to u_s .

Also, from (21), we have:

$$I_{s1} \cos\varphi_1 = I_{s2} \cos\varphi_2 = I_{s3} \cos\varphi_3 = I_s \cos\varphi. \quad (31)$$

From (31) and Figure 10 we see that the trajectory of i_s will slide perpendicular to u_s .

Increasing the excitation source from E_{q1} to E_{q3} causes the phase angle of the current with voltage to change from phase lag state to phase lead state. The value of the excitation source that produces the normal power factor is called the normal excitation. Excitement higher than the normal value is typically called over-excitation. In this scenario, the motor works as a synchronous compensator. Excitement lower than the normal value is called under-excitation. In this case, the

engine works like an asynchronous machine. The above analysis shows that power factor correction is beneficial in applications where the motor is subjected to high transient loads. The power factor regulator must measure the power factor drop that occurs when the motor is subjected to a sudden heavy load and send a signal to the thyristor static rectifier to increase the value of the excitation source. This process is called excitation enhancement. As a result, the pull-out torque of the synchronous motor is increased during transient loads. After the load drops, the regulator senses the excessive lead-in power factor and drives the rectifier to drop the voltage at its output. Another application of the power factor regulator is to control the variation of the plant power factor caused by other loads such as asynchronous motor running under or no load, thereby improving the voltage quality of the plant.

III. CONTROLLER DESIGN

The structure diagram of the excitation control system, using hybrid PI-FLC control, is shown in Figure 11.

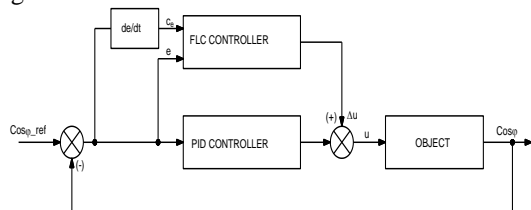


Figure 11. Hybrid PI-FLC Sugeno controller.

In this diagram, the object consists of a three-phase 6 pulse bridge rectifier and the synchronous motor. The output voltage of the rectifier will provide a field source for the rotor windings. The power factor $\cos\phi$ is measured at the stator side of the motor and compared with the setpoint. The error $e(t)$ is fed to the PI controller for processing. The fuzzy controller receives the error signal $e(t)$ and its derivative to process according to the established composition rule. The output signal of the PID controller and fuzzy logic controller is added and sent to the thyristor excitation regulator to change the DC output voltage of the rotor winding.

3-1- PI controller design

The initial parameter of the PI controller was determined by Ziegler-Nichols. The steps are as follows:

Let the system work in closed loop with the proportional controller P. Set the components I (integral) and D (derivative) to 0.

Let the system work in closed loop with the proportional controller P. Set the components I (integral) and D (derivative) to 0.

Step 1: Increase the value of K_p

Step 2: Increase K_p until the system stops harmonic oscillation, note that this increase is K_{cr}

Step 3: The system oscillates with period P_{cr} (P_{cr} is measured in seconds) as shown in Figure 12.

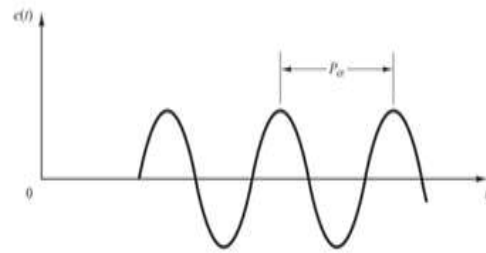


Figure 12. Harmonic oscillation function with period P_{cr}

Step 4: The parameters K_p , T_i and T_d are determined as in Table 1.

Table 1. Ziegler-Nichols 2 method for PID controller parameter determination

Controller type	K_p	T_i	T_d
P	$0.5K_{cr}$	∞	0
PI	$0.45K_{cr}$	$\frac{1}{1.2}P_{cr}$	0
PID	$0.6K_{cr}$	$0.5P_{cr}$	$0.125P_{cr}$

After determining the PI controller parameter by Ziegler-Nichols, the trial and error method is performed to further refine, the steps are as follows:

Step 1: Set the Setpoint value.

Step 2: Keeping K_i value and adjusting K_p with 25% increments, determine the value of K_p for the best response.

Step3: Keep the K_p value determined in step 2 and adjust K_i with a 25% increment, determining the value of K_i for the best response.

Step4: The controller parameter pair is the K_p and K_i values determined in steps 2 and 3.

3-1-Fuzzy controller design

In this study, the combination of fuzzy controller and PI controller to create a hybrid fuzzy controller is used to control excitation for synchronous motor. A cascade hybrid fuzzy structure is shown in Figure 11.

The fuzzy controller will have 2 inputs and 1 output, shown in Figure 13. The membership

functions for the input/output of the fuzzy controller are shown in Figure 14.

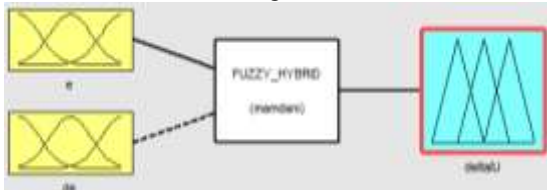


Figure 13. Input/output structure of fuzzy controller in hybrid fuzzy system



Figure 14a. The membership functions e(t)



Figure 14b. The membership functions de(t)/dt

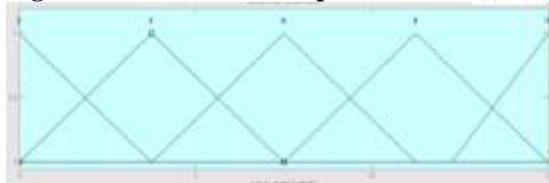


Figure 14c. The membership functions Δu

In the structure of Figure 13, the first input of the fuzzy controller is “e”, which is fuzzy by 5 membership functions {NB, NS, Z, PS, PB} and the second input is “de”, which is fuzzy by 5 membership functions {NB, NS, Z, PS, PB} (Figures 14a and 14b). The membership functions of the input fuzzy sets used are (trimf) and (trmf).

The domain of the input variable is defined as follows:

$$e = [-1 \ 1]; \quad de = [-1 \ 1]$$

The output of the fuzzy controller is “ Δu ”, which is fuzzy by 5 membership functions {Z, S, M, B, VB} (Figure 14c). In this study, the output variable is determined to be an offset for the control signal 0 - 15V corresponding to the main signal supplied to the rectifier circuit.

$$\Delta u = [0 \ 15]$$

In which, the variables are explained as follows: “N” is “Negative”; “Z” is “Zero”; “P” is “Positive”; “S” is “Small”; “B” is “Big”; “VB” is “Very Big”. The fuzzy rule is selected as MAX-MIN and the defuzzification is done by the center point method. The rule of fuzzy controller is determined according to table 2.

Table 2. Table of control rules

Δu		e				
		NB	NS	Z	PS	PB
de	NB	S	M	Z	B	VB
	NS	S	M	Z	B	VB
	Z	S	M	Z	B	VB
	PS	S	M	Z	B	VB
	PB	S	M	Z	B	VB

IV. SIMULATION RESULTS AND DISCUSSION

The simulation is done on matlab - Simulink with the synchronous motor when it has been started and is working at steady state, taking into account the change of load. The simulation parameters are given in Table 3. The simulation diagram is presented as shown in Figure 15.

Table 3. An example of a table.

Parameter	Symbol	Value	Unit
Stator resistance	R_s	0.26	Ω
Stator leakage inductance	$L_{s\sigma}$	1.14	mH
d-axis magnetising inductance	L_{md}	13.7	mH
q-axis magnetising inductance	L_{mq}	11	mH
d-axis damper winding resistance	R_D	0.0224	Ω
d-axis damper winding leakage inductance	$L_{D\sigma}$	1.4	mH
q-axis damper winding inductance	R_Q	0.02	Ω
q-axis damper winding leakage inductance	$L_{Q\sigma}$	1	mH
Number of pair of poles	p	10	-

Magnetising winding resistance	R_f	0.13	Ω
Magnetising winding leakage inductance	$L_{f\sigma}$	2.1	mH
Rate stator current of phase A	I_a	53.9	A
Rate Stator current of phase B	I_b	53.9	A
Rate Stator current of phase C	I_c	53.9	A
Initial phase A of the current	ph_a	-173.3	Degree
Initial phase B of the current	ph_b	66.7	Degree
Initial phase C of the current	ph_c	-53.3	Degree
Rate excitation source	E_q	17.8876	V

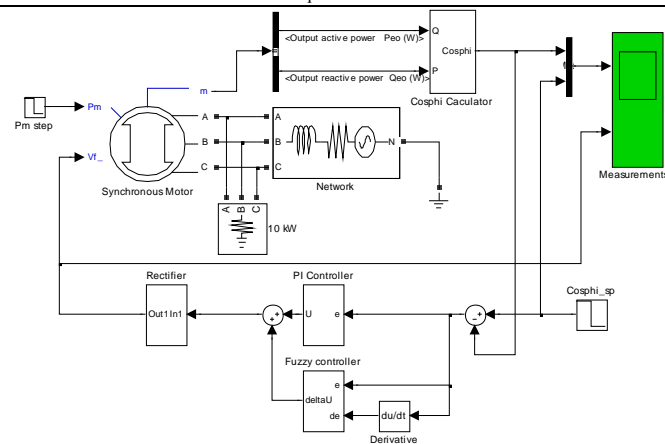


Figure 15. Matlab simulation diagram – Simulink

To evaluate the quality of synchronous motor excitation control system. We compare:

1. Using the PI controller, the controller parameters are determined by the Ziegler-Nichols method.
2. Using the PI controller, the controller parameters are determined by the Ziegler-Nichols method combining Trial and error.
3. Using hybrid fuzzy control system with PI controller

The simulation results are presented as shown in Figures 16 and 17.

From the simulation results, we can make a comparison table as shown in tables 4 and 5.

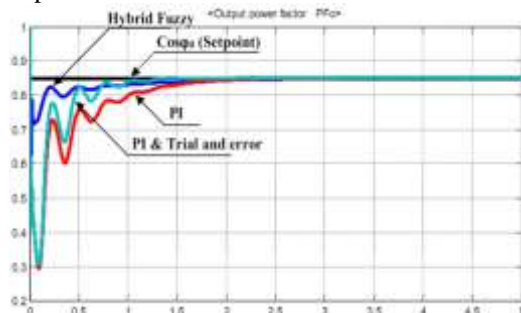


Figure 16. The response when the load is constant

Table 4. Quality comparison table of controllers under constant load

Comparison criteria	Controller		
	Hybrid	PI & trial error	PI
overshoot (%)	0	0	0
Transition time (s)	1	1.5	1,8
Stable time (s)	1.7	2.2	2,7
Error (%)	0	0	0

According to Table 4, the hybrid fuzzy controller gives the best response.

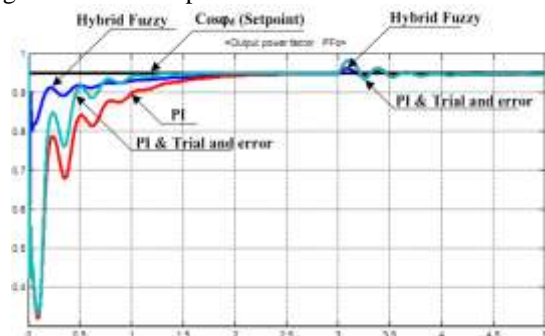


Figure 17. The response when the load changes

Table 5. Quality comparison table of controllers when the load changes

Comparison criteria	Controller		
	Fuzzy Hybrid	PI & trial error	PI
overshoot (%)	1	3,2	3,2
Transition time (s)	0,4	0,7	0,8
Stable time (s)	0,75	1,5	1,5
Error (%)	0	1,5	1,5

V. DISCUSSION:

A hybrid control system between fuzzy controller and PI controller is proposed to control excitation for synchronous motor. Simulation results show that the use of hybrid fuzzy control system gives the best response quality, even when there is a change in load. Therefore, it is possible to propose a hybrid fuzzy system between fuzzy controller and PI controller for excitation control system of power synchronous motor, when describing transfer function of synchronous motor is difficult.

REFERENCES

- [1] D P Kothari and I J Nagrath; "Electric machine"; TMH Publishers second edition, 1998.
- [2] M. G. Say; "Performance and design of ac machine"; CBS Publishers third edition, 2002.
- [3] DR. P.S. Bimbrha; "Electrical Machinery"; Khanna Publisher seventh edition; 2009.
- [4] Bill Horvath; "Synchronous Motors & Sync Excitation Systems", Western Mining Electrical Association; TM GE Automation Systems, 2009.
- [5] Al-Hamrani MM, Jouanne AV, Wallace A; "Power factor correction in industrial facilities using adaptive excitation control of synchronous machines"; Conference Record of the 2002 Annual Pulp and Paper Industry Technical Conference; 2002 June, 17-21; Toronto, Canada: 148-154.
- [6] WEG group; "The ABC's of Synchronous Motors"; At https://www.electricalmachinery.com/files/LR10012.gb.0111.01_SynchMotors_Mining.pdf
- [7] Sittipong Pengpradern, Kreangsuk Kraikitrat, Somporn Ruangsinchaiwanich; "Automatic control of synchronous motor using PI controller for improving power factor"; Journal of Thai Interdisciplinary Research; Volume 12, Number 5, Pages 35 – 41; 31 October 2017
- [8] Maamoon F. Al-Kababji , Ahmed Nasser B. Al-Sammak; "Modeling & simulation of synchronous machine controlled by PID control for the reactive power compensation"; The 6th Jordanian International Electrical & Electronics Engineering conference JIEEEEC 2005.
- [9] Arş. Gör. E. Kılıç, andI. H. Altaş; "Power Factor Correction of Synchronous Motor Using Fuzzy Logic"; Mathematical and Computational Applications. 1996; 1(1):66-72. at <https://www.mdpi.com/2297-8747/1/1/66>
- [10] Ahmet Gani, Ö. Fatih Keçecioglu, Hakan Açıkgoz, Ceyhun Yıldız, Mustafa Şekkeli; "Simulation Study on Power Factor Correction Controlling Excitation Current of Synchronous Motor with Fuzzy Logic Controller"; International Journal of Intelligent Systems and Applications in Engineering, ISSN:2147-6799, IJISAE, 2016, 4(Special Issue), 229–233.
- [11] T. Anitha; G. Gopu; M. Nagarajapandian; P. Arun Mozhi Devan; "Hybrid Fuzzy PID Controller for Pressure Process Control Application" ; 2019 IEEE Student Conference on Research and Development (SCORED); DOI: 10.1109/SCORED.2019.8896276
- [12] T. Brehm; K.S. Rattan; "Hybrid fuzzy logic PID controller"; Proceedings of 1994 IEEE 3rd International Fuzzy Systems Conference; DOI: 10.1109/FUZZY.1994.343602;
- [13] A.H.Gomaa Haroun; Yin-yaLi; "A novel optimized hybrid fuzzy logic intelligent PID controller for an interconnected multi-area power system with physical constraints and boiler dynamics"; ISA Transactions; Volume 71, Part 2, November 2017, Pages 364-379.
- [14] Isin Erenoglu, Ibrahim Eksin, Engin Yesil, Mujde Guzelkaya; "An Intelligent Hybrid Fuzzy Pid Controller"; Conference: ECMS-2006, 20th European Conference on Modelling and Simulation At: Bonn, Germany, 2016; DOI:10.7148/2006-0062
- [15] J.P.Torreglosa; Jurado; García; M.Fernández; "Application of cascade and fuzzy logic based control in a model of a fuel-cell hybrid tramway"; Engineering Applications of Artificial Intelligence;



- Volume 24, Issue 1, February 2011, Pages 1-11.
- [16] Jukka Kaukonen. "Slitent pole synchronous machine modelling in an industrial direct torque controlled driver application." Thesis for the degree of doctor of science technology, Lappeenranta (1999); ISBN 951 – 764 – 305 – 5; ISSN 1456 – 4491.
- [17] Bui Quoc Khanh, Doan Quang Vinh, Pham Quang Dang, Nguyen Quang Dich. "Industrial electric drive control."; Scientific and technical Publishers (2020).